

LIU Wei-min, YAN Yong-li, LIU Kang-jun, XU Chun-he,  
QIAN Shi-xiong

## The study of photo-induced ultrafast dynamics in light-harvesting complex LH2 of purple bacteria

© Higher Education Press and Springer-Verlag 2006

**Abstract** In this paper, we introduce the photo-induced ultrafast dynamics taking place in the peripheral light harvesting antenna LH2 from purple bacteria *Rhodospirillum rubrum* by using absorption, fluorescence emission and ultrafast spectroscopic techniques. Three kinds of LH2 samples, pH treated LH2 (complete removal of B800 pigments), carotenoid mutated LH2 (GM 309) and electrochemical oxidation treated LH2 were used in comparison with native LH2 to investigate the mechanism of photo-induced ultrafast energy transfer within the LH2 complex.

**Keywords** bacteria, photosynthesis, light-harvesting antenna, femtosecond pump-probe, energy transfer

**PACS numbers** 34.30.+h, 42.65.Re, 78.47.+p

### 1 Introduction

Life on Earth ultimately depends on the collected energy emitted by the Sun. Photosynthesis is the only process of biological importance that can harvest this energy. Photosynthetic organisms use solar energy to synthesize organic compounds, e.g., carbohydrates, that cannot be formed without input of energy. Energy stored in these molecules can be used later to power cellular processes and can serve

as energy source for all forms of life.

Although the photosynthetic process in various photosynthetic systems (plant and bacteria) might show some differences, the primary process in all photosynthetic systems is the ultrafast photophysical process which happens in the antenna and reaction center (RC) [1–3]. The solar energy is first absorbed by the antenna, the pigment-protein complexes that are generally located in the membrane of the system and contain molecules such as bacteriochlorophylls/chlorophylls (BChls/Chls) and carotenoids (Cars). These molecules can absorb the light energy in different regions of the solar spectrum from 400 nm to 1 050 nm, leading to an increased light absorption efficiency of the system [4], which is determined by their chemical structure and is drastically affected by the interactions with their environment. The excitation energy in the light harvesting antenna would be transferred to RC, leading to the charge separation in the reaction center and the subsequent complicated physical and chemical processes.

In the antenna, the absorption of light leads to the excitation of the excited state in pigments. Energy transfer of the excitation between the closely packed pigments occurs on ultrashort timescales, ranging from subpicoseconds (hundred of femtosecond) to picosecond (ps) and eventually the excitation ends up in the reaction center (RC), the special pigment-protein complex responsible for the charge separation [4]. The initial light energy is stored in a transmembrane electrochemical gradient that drives the formation of energy compounds like adenosine triphosphate (ATP), which can be used later for biochemical synthesis in the cell.

Investigating the dynamics of the different primary processes in (bacteria) photosynthesis, which range from tens of femtoseconds ( $1 \text{ fs} = 10^{-15} \text{ s}$ ) to picoseconds (ps), is a very important and attractive task that has been greatly driven by the technological developments during past decades. After the invention of the first ruby laser, an enormous variety of laser systems has been developed, which cover quite a broad

LIU Wei-min, YAN Yong-li, LIU Kang-jun, QIAN Shi-xiong (✉)  
Physics Department, Fudan University, Shanghai 200433, China  
E-mail: sxqian@fudan.ac.cn

XU Chun-he  
Shanghai Institute of Plant Physiology & Ecology, Shanghai Institute  
for Biological Sciences, Chinese Academy of Science,  
Shanghai 200032, China

Received April 10, 2006

spectral range and very wide scale of the pulse duration, from continuous laser beam to the ultrashort laser pulses. The significant success in building the picosecond and femtosecond laser dramatically stimulated the research of the ultrafast energy transfer process in the primary process in photosynthesis, leading to the better understanding of the primary process. Nowadays, most ultrafast experiments are based on the use of Ti: sapphire laser which allowed the study of dynamics on a femtosecond timescale. The utilization of the ultrashort pulses greatly improves the precision with which the dynamics of the primary process can be studied, and the ultrafast spectroscopic techniques are being widely used in the study of photosynthesis and photobiology field.

In this paper, we introduce our research work on the ultrafast dynamics that happen in isolated LH2 complex of purple bacteria. In Sect. 2, we review the experimental setup of femtosecond pump-probe measurement. Section 3 is the introduction of photosynthetic unit of purple bacteria. In Sects. 4, 5 and 6, three kinds of treated or mutated LH2 samples were compared with native LH2 to investigate the mechanism of energy transfer among B800, B850 and carotenoid pigments within the LH2 complex. A summary is given in Sect. 7.

## 2 Femtosecond pump-probe measurement

The femtosecond pump-probe technique is a very useful technique in studying the ultrafast response of different kinds of the materials, including polymers, condensed matters, atoms and molecules, and the biological systems. The ex-

perimental setup of the femtosecond pump-probe is shown in Fig. 1. The principle of pump-probe is that when an intense ultrashort laser beam (pump beam) is incident on the sample to be studied, it may induce some changes in the electronic and/or optical properties of the sample. For detecting the photo-induced changes in the sample, another weak beam (probe beam) is used to incident on that spot of the sample. Due to the change of the optical properties of the sample under the action of the pump beam, the transmittance and the refractive index of the sample are different from those of the unperturbed material. Hence, the change of the transmittance, or the differential absorption, carries a lot of information about the processes occurring in the material. For measuring the dynamic response, an optical delay line (ODL) is used to generate the optical delay between pump and probe beams, which can easily control the optical delay within 10 fs and is now widely used in the measurement of the ultrafast response in the fs domain. To increase the signal to noise ratio (SNR), lock-in amplifier is commonly used and a chopper is inserted in the path of the pump beam. The output from the lock-in amplifier is the differential absorption signal of the sample [5].

In our experiment, femtosecond pump-probe measurements were carried out by using a Spectra Physics Ti: sapphire laser at room temperature. In one color configuration, the output fs pulses from the oscillation stage were used, which had the pulse duration of about 120 fs, repetition rate of 82 MHz and the tunable range from 760 nm to 860 nm. The average pump power incident on the sample is about 30 mW, and the ratio of the intensity between the pump and probe beam is about 8:1. Two color pump-probe measurements were taken by using the output from an am

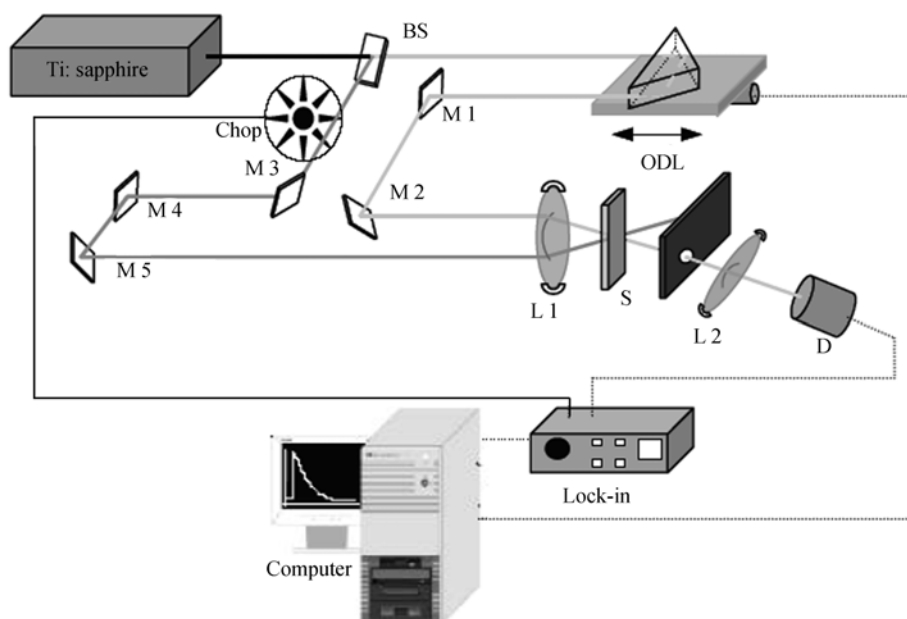


**Fig. 1** Experimental setup of femtosecond pump-probe measurement. Where BS is beam splitter; M1 — M5 are mirrors; L1, L2 are lenses; ODL is optical delay line; S is sample; A is aperture; D is detector.

plifier stage with 1 kHz repetition rate, 140 fs pulse duration and 800 nm central wavelength. The laser output was split by a beam splitter into two beams, one was used as the pump beam and the other was utilized to generate a super-continuum from which the wavelength of the probe beam was selected by a monochromator.

### 3 Photosynthetic unit of purple bacteria

The purple bacterial photosynthetic units are simpler than those of plants, and they generally consist of only one type of RC and two types of antennae, Light-harvesting 1 (LH1) and Light-harvesting 2 (LH2). Both the peripheral LH2 and LH1 antenna of purple bacteria, are characterized by a high degree of symmetry, nine-fold [6,7] or eight-fold [8], respectively. In Fig. 2, a typical spatial arrangement of the purple bacterial photosynthetic complexes is shown, the reaction center is surrounded by the core antenna LH1, and outside the RC-LH1 complex lies the peripheral antenna LH2. The excitation energy is captured by a pigment in the LH2 complex and is transferred between a number of LH2s before eventually ending up, via the LH1, in the RC. Here, we mainly focus on the function and dynamics of LH2 complex. The structure of LH2 had been determined at 0.24 nm resolution [6] and is shown in Fig. 3 (a). It is characterized by nine-fold axial symmetry, with two  $\alpha$ -helical polypeptides, three bacteriochlorophylls *a* and one (or possibly two) carotenoid per unit. LH2 has two parallel rings of Bchl molecules, giving rise to  $Q_y$  absorption band located at 800 nm (B800 band) and 850 nm (B850 band), which are caused

by the different pigments, denoted as B800 and B850, respectively. The B800 band originates from 9 quasisymmetric Bchl molecules that have their planes parallel to the membrane surface, the large distance of 2 nm adjacent B800 Bchl molecules leads to a weak interaction energy of  $\sim 20 \text{ cm}^{-1}$ . The B850 band originates from 18 strongly interacting Bchl molecules with their planes perpendicular to the membrane surface. The much shorter distance of about 0.9 nm between neighboring B850 Bchl molecules leads to large interacting energy of  $\sim 250\text{--}300 \text{ cm}^{-1}$  [9–11].

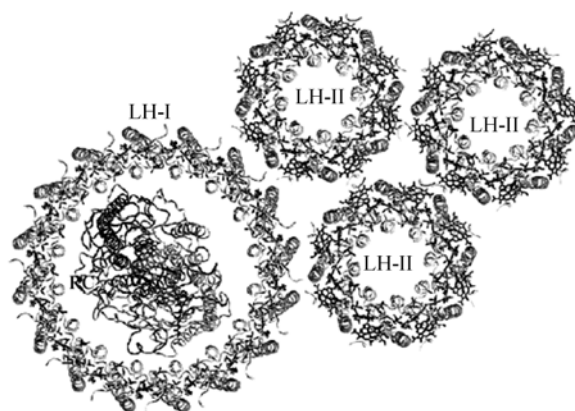


Fig. 2 Model for the photosynthetic unit of purple bacteria.

The absorption spectra of LH2 complexes are shown in Fig. 3 (b). There are carotenoids absorption bands at 512, 479 and 451 nm corresponding to different vibronic bands, and typical B800 and B850 bands are at 800 and 850 nm, respectively. In the LH2 complex, under photoexcitation of

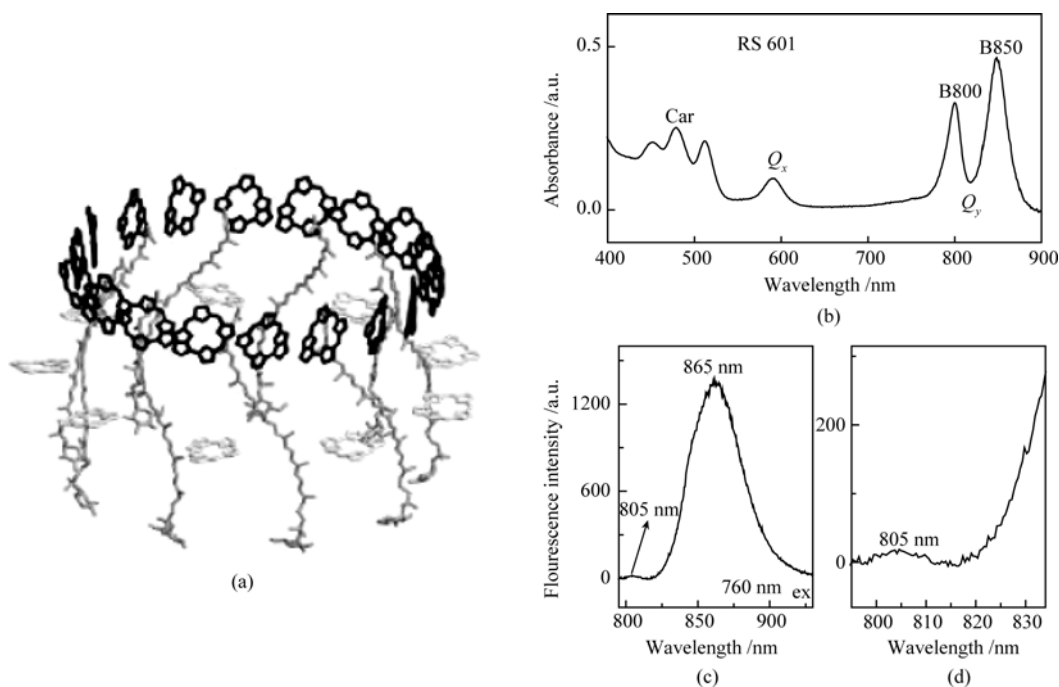


Fig. 3 (a) Structure of LH2 ring. (b) absorption spectrum of LH2 at room temperature. (c) and (d) Fluorescence emission spectra of the LH2 under excitation at 760 nm.

B800 pigments, the excitation energy can be transferred from B800 to B850 pigments. In native bacteria photosynthetic system, the excitation of B850 pigment would be transferred to LH1 and finally to RC, but in isolated LH2 complex, this excitation would be finally dissipated via fluorescence emission from B850. The fluorescence emission spectra of the LH2 complexes upon photoexcitation of B800 pigments are shown in Fig. 3 (c) and (d). Under the excitation of 760 nm, a strong fluorescence emission at 865 nm is detected, which originates from the spontaneous emission of B850 pigments. Moreover, a weak emission peak located at 805 nm is also observed, which comes from the spontaneous emission of B800 pigments.

Three kinds of samples used in the experiment are described in the following:

(i) The native LH2: *Rhodobacter sphaeroides* (RS601) was grown anaerobically at 30°C in Sistrom's minimal medium. Cells were collected by centrifugation. After cells were ruptured using an ultrasonifier, chromatophores were isolated with high-speed centrifugation. Finally, chromatophores were solubilised by using LDAO and LH2 complexes were purified by using DEAE-cellulose chromatography.

(ii) The LH2 complexes with completely removed B800: LH2 complexes were acidified by plus acetic acid in LM buffer (0.01 mol/L Tris-HCl, 0.01 mol/L *n*-dodecyl- $\beta$ -maltosid, 0.005 mol/L ascorbic acid pH 8.0). After incubation for 30 min at pH 3.6, the absorption spectra of sample were detected. To remove free BChl, chromatographs were performed on DEAE-cellulose 52. The chromatographs were performed on a FPLC and eluted components were monitored by absorbance at 280 nm. Afterwards, pH was adjusted back to 8.0 with NaOH. Finally, we acquired the LH2 complex with completely removed B800 (called B850p).

(iii) The carotenoid mutated LH2: GM309, a special green mutant strain (GM309) was obtained by ethylmethane sulfonate (EMS) induced mutagenesis from *Rb. sphaeroides* 601 (RS601). HPLC-Mass analysis of carotenoids showed that the neurosporene was accumulated in LH2 of GM309 [12]. In our experiments, the mutation frequency of pigment mutants in surviving cells is  $1.6 \times 10^{-3}$ . In organisms with such a low mutation frequency, it is unlikely to find double mutants of both apoproteins and carotenoids.

#### 4 Energy transfer within the LH2 complex

Excitation of the B800 band in the isolated LH2 complex is followed by energy transfer processes between the B800 pigments, from B800 to B850, between the B850 pigments and eventually by decay of the excited state of B850. Intermolecular excitation transfer among weakly coupled B800 molecules or from B800 to B850 is generally described by the Förster hopping mechanism [10, 13–15], while exci-

tonic character of the excited state has been identified in B850 band, where the excitation is delocalized over a number of B850 pigment molecules due to the strong pigment-pigment interaction and the dynamics take place through relaxation among different excitonic states in the B850 ring [13–18]. Theoretical calculated spectroscopic properties of the B850 ring in LH2 indicate that the absorption transition in B850 can span over the spectral region from 780 to 880 nm [19]. According to the excitonic model, the major absorption near 850 nm is due to two degenerate delocalized excitonic levels ( $k = \pm 1$ ), while transition from the ground state to the lowest excitonic level ( $k = 0$ ) is formally forbidden. Because of the energetic and structural disorder effect, the originally degenerate excitonic levels may be distorted, leading to the possible transition to all these excitonic levels [20].

The ultrafast energy transfer between B800 pigments, B800→B850 and between B850 pigments have been widely studied with various techniques, such as femtosecond pump-probe [21, 22], femtosecond transient absorption [23, 24] and transient grating techniques [25]. For B800-B850 energy transfer, it was found that the excitation energy in B800 pigments can be efficiently transferred to B850 with a time of  $\sim 0.7$  picosecond at room temperature and 1.2 ps at 77 K [26, 27]. The fs pump-probe dynamics of LH2 complex at 800 nm is given in Fig. 4 (a). Under excitation of 800 nm beam, the LH2 complex shows a dominated transient photobleaching (PB) signal and an additional photoabsorption (PA) appeared at delayed time, which is attributed to the excited state absorption of B850 pigments. The ultrashort decay time of the PB signal was determined to be about 650 fs which mainly reflects the energy transfer rate from B800 to B850 pigments.

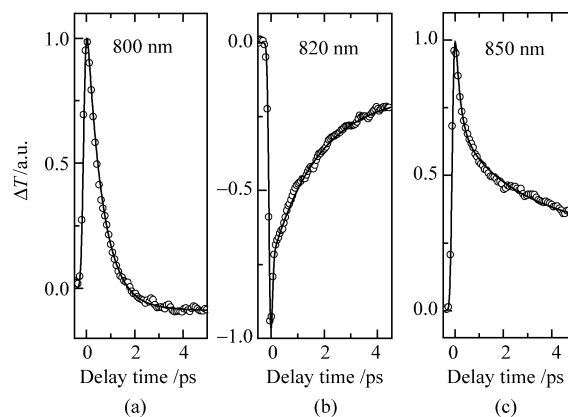


Fig. 4 Normalized one color fs pump-probe dynamics of LH2 at (a) 800 nm, (b) 820 nm and (c) 850 nm. The solid lines represent the fitting results.

When the laser wavelength was tuned from 820 nm to 850 nm, the main excitation was in the B850 band. The experimental results clearly demonstrate the evolution of the excited B850 pigments and the obvious excitation wavelength dependence was observed. The dominated PB or PA signal at different wavelengths depends on the absorption

cross-sections of the ground state and the excited state as well as on the populations in different excited states, and the photodynamics of LH2 complex. The dynamics of native LH2 at 820 and 850 nm are shown in Fig. 4 (b) and (c), respectively. Under the excitation at 850 nm, the dynamics consist of an initial ultrafast decay of the PB and a long-lived decay component. Three time constants of  $\sim 200$  fs,  $\sim 2$  ps and  $> 100$  ps are obtained from the data fitting, which reflects the intra / interband energy transfer pathways in the B850 ring [28]. Moreover, the longest time constant that corresponds to the long lifetime of the lowest excitonic level of B850 ( $\tau \sim 1$  ns [29]) cannot be accurately fitted from the data because of the relatively short time window.

For the dynamics of B800–B850 energy transfer, calculations based on the conventional Förster theory cannot perfectly explain the experimentally measured transfer times [14,15]. It was suggested that some factors in the calculations were underestimated, such as the spectral overlapping of B800 with upper excitonic levels of B850 ring, the other factor comes from the additional electronic coupling mediated by carotenoids, which will be introduced at Sect. 5. Theoretically calculated spectroscopic properties of the B850 ring in LH2 indicated that the absorption transition in B850 spans over the range from 780 to 880 nm [19]. In that case, the upper excitonic levels of B850 band, lying in the vicinity of the B800 band, might play a role in the relaxation dynamics under the excitation near 800 nm [30, 31]. Moreover, by using the different B800-released LH2 complexes, the characteristics of upper excitonic levels of B850 band have been directly observed by circular dichroism spectra, nonlinear absorption and ultrafast pump-probe techniques [32, 33].

Figure 5 shows the absorption spectrum of B850p. The absorption peak of B850 band in B850p is red-shifted about 1.5 nm compared with that of native LH2 as a result of the deletion of B800 pigments [30], and the absorption band of B800 completely disappears due to the total removal of B800 pigments. The BChl-B800 molecules were released through acidification, which indicates that the interactions between BChl-B800 molecules and apoproteins are sensitive to pH values. B850 molecules are arranged tightly between  $\alpha$  and  $\beta$  by forming hydrogen bonds between BChl-B850 and  $\alpha$ -Trp45-NE1 or  $\alpha$ -Tyr-44-OH [34]. There is a coordinate linkage between the  $Mg^{2+}$  of BChl-B850 and histidine residue ( $\alpha$ His31, $\beta$ His30). The unchanged  $Q_y$  transition peaks of B850 exhibit that the interactions between BChl-B850 molecules and apoproteins are nearly not affected by acidification with different pH values.

When the excitation wavelength was at 800 nm, for B850p with completely released B800 pigments, the dynamics exhibit a dominated PA signal (see Fig. 6) instead of the PB signal observed in native LH2 complexes [35]. The PA decay process comes from the excited-state absorption of upper excitonic levels of B850 band under the direct optical excitation [36]. It is proposed that the mixed PA and PB behaviors of the LH2 complexes are closely related to the contribution of the excited states in both B800 and B850 pig-

ments around 800 nm. Because the absorption cross section of the first excited state in B800 pigments is smaller than that of the ground state, B800 pigments produce a PB signal in the pump-probe dynamics. On the other hand, as the absorption cross section of the high lying excitonic levels is larger than that of the ground state for B850 pigments, the transient behavior demonstrates a PA signal.

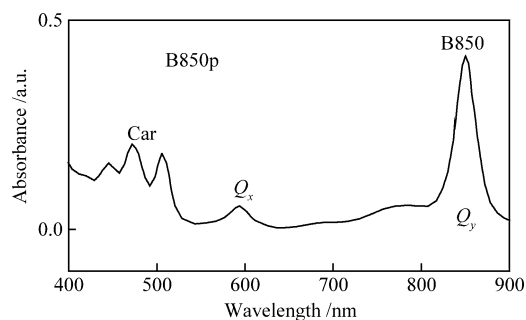


Fig. 5 Absorption spectrum pH treated LH2 (B850 p) at room temperature.

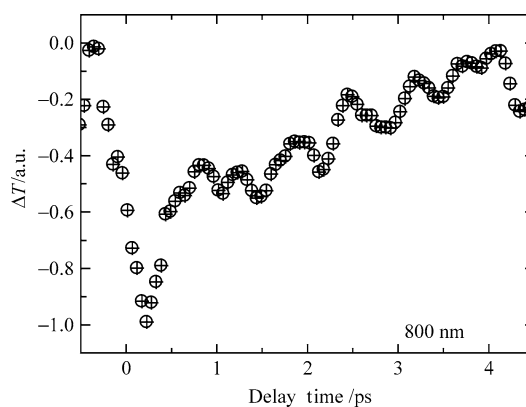


Fig. 6 Normalized one color fs pump-probe dynamics of B850 p at 800 nm.

When the laser wavelength was tuned from 820 nm to 850 nm, The dynamics of B850 p at 820 and 850 nm shows the similar dynamical behavior as compared with that of native LH2 (as shown in Fig. 7). It is considered that al-

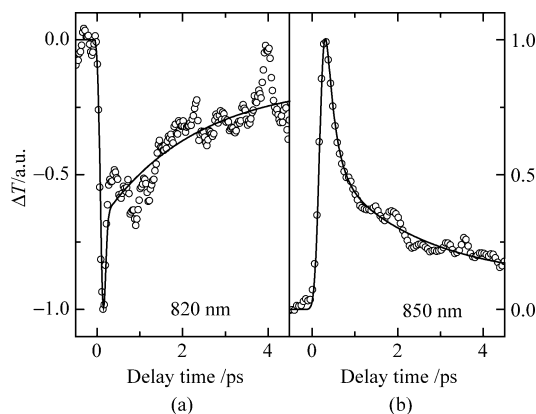


Fig. 7 Normalized one color fs pump-probe dynamics of B850 p at (a) 820 nm and (b) 850 nm. The solid lines represent the fitting results.

though the deletion of B800 pigments results in a small red shift of B850 band in B850 p, the coupling of the B850 pigments in the ring is not significantly affected [29]. In that case, in the range between 820 nm and 850 nm, the fs dynamics of two kinds of LH2 complexes would be similar, mainly reflecting the effect of B850 pigments [30, 33].

## 5 How carotenoid affect the energy transfer within the LH2 complex

One of the most important constituents in the light harvesting LH2 of many photosynthetic systems is the carotenoid. The diverse roles played by carotenoids in light-harvesting complexes, including light harvesting, photoprotection, and structure stabilization [37–39], are directly related to the efficiency and viability of the photosynthetic systems. In the bacterial light-harvesting systems, light absorbed by carotenoids is transferred via singlet–singlet interaction to B800 and B850 bacteriochlorophylls (BChl) in the ratio 25 % to 75 % [40–42]. As we mentioned above, for the B800–B850 energy transfer, the commonly used Förster theory provides an unsatisfactory estimate of the energy transfer efficiency. The effect of the carotenoid on the energy transfer between B800 and B850 can be compared to that in donor-bridge-acceptor systems. By using quantum chemical calculations, it was suggested that the transition densities of both the B800 and B850 BChls are perturbed by interaction with the bridging carotenoids and that the B800–B850 coupling is increased by approximately 20 %–30 % via mixing of the BChl and carotenoid transition moments [43].

Recently, different kinds of mutated carotenoids with extended  $\pi$ -electron conjugation systems ranging from seven to thirteen carbon-carbon double bonds were studied by time-resolved transient absorption. Results revealed that the lifetime of the S1 state of these carotenoids is decreased with the increasing conjugation length [44]. In this section, we discuss how carotenoids with different conjugation lengths affect the ultrafast dynamic processes of energy transfer in LH2. The carotenoid mutated LH2 complexes (called GM 309) containing nine carbon-carbon double bonds carotenoids (neurosporene) were studied in comparison with the native LH2 containing ten carbon-carbon double bonds carotenoids (spheroidene) (see Fig. 8). The experimental results exhibit remarkably different B800→B850 energy transfer behaviors.

The absorption spectra of two LH2 complexes, native LH2 and GM309, are shown in Fig. 9. In the near-infrared region, both spectra are dominated by characteristic features due to the  $Q_y$  bands of BChl, with peak wavelengths of the B800 and B850 at 800 nm and 850 nm for both LH2 samples. In the 400–550 nm region, due to the vibronic bands of carotenoids, a typical three-peak absorption feature dominates the absorption spectrum of native LH2. A sig-

nificant blue shift of  $\sim 20$  nm of the three carotenoid peaks was observed in GM309, because of the higher energy levels of neurosporene with nine carbon-carbon double bonds as compared to those of spheroidene with ten carbon-carbon double bonds [44, 45].

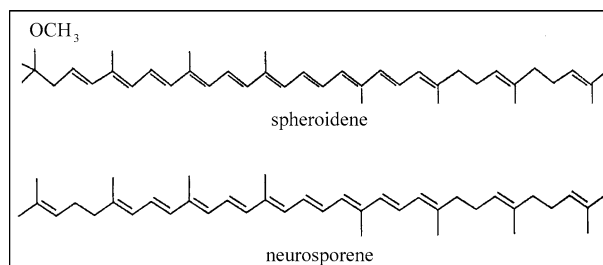


**Fig. 8** Molecular structure of the carotenoids (Cars).

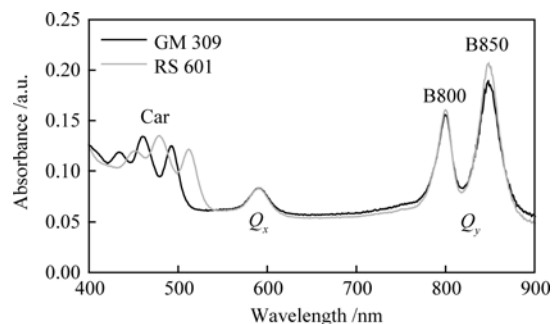


**Fig. 9** Absorption spectra of LH2 complexes: wild-type LH2 containing spheroidene (*gray line*) and green carotenoid mutated GM309 containing neurosporene (*black line*).

The fluorescence emission spectra of the two LH2 complexes upon photoexcitation of B800 pigments are shown in Fig. 10. The intensity of the fluorescence emission from B850 of GM309 is 40 percent of that of native LH2, which reveals that the energy transfer from B800 to B850 is partly blocked by the carotenoid mutation and that nonradiative relaxation processes may play a crucial role in the mutated LH2 complex.

The one color fs pump-probe results of native LH2 and GM309 at 800 nm are given in Fig. 11. Under excitation at

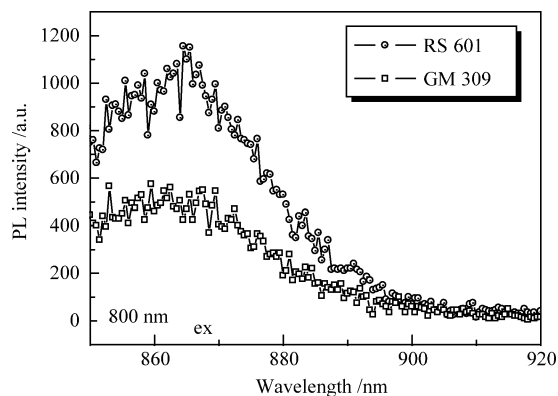


**Fig. 10** Fluorescence emission spectra of the native LH2 and GM 309 under excitation at 800 nm.

800 nm, the decay time of the PB signal, which mainly reflects the energy transfer rate from B800 to B850, is dramatically increased in GM309 (870 fs) in comparison with that in native LH2 (650 fs). It has been postulated that the discrepancy between the experimentally measured and the calculated energy transfer rates from B800 to B850 may partly come from the mediated coupling via the carotenoids [14, 43]. It has been recently reported that singlet-singlet energy transfer rates are increased by through-band exchange interaction [46–48]. In particular, the work of Kilsa *et al.* [46] highlighted an expected increased electronic energy transfer rate for the decreased energy separation between the singlet excited state of donor and bridge. Based on our experimental results, we suggest that the energy transfer rate between B800 and B850 in GM309 could be decreased due to the fact that neurosporene, containing nine carbon-carbon double bonds, induces a relatively higher band gap between the B800 donor and the carotenoid bridge as compared to that in native LH2.

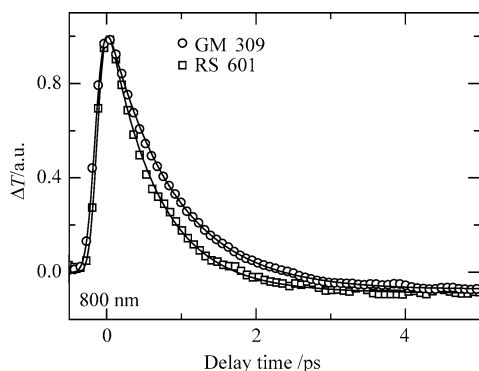


**Fig. 11** Normalized one color fs pump-probe dynamics of the native LH2 and GM 309 at 800 nm. The solid lines represent the fitting results.

Two color fs pump probe measurements were also carried out with the probe beam at 860 nm under excitation at 800 nm. The results are shown in Fig. 12. Excitation of B800 pigments results in the transient dynamics of B850 pigments with a fast rise of photobleaching and a slow decay process. The fast rise component comes from the energy transfer from B800 to B850 and the cross correlation between the pump and the probe beams. In that case, the slower rising time constant for GM309 reflects the decreased B800 → B850 energy transfer rate as compared to that in native LH2. Fitting results by rate equations for the LH2 system show that the first half of the rising edge is mainly contributed by the cross correlation between the pump beam and the probe beam, while the latter part reflects the B800 → B850 energy transfer process. The decay process reflects the relaxation of the excited B850 pigments, via both the radiative and nonradiative processes. Time-resolved fluorescence measurements of these two samples (see Fig. 12) show that B850 with a fluorescence lifetime of  $1\,026 \pm 50$  ps for GM309 is very similar to that of the native LH2 of  $1\,060 \pm 50$  ps. It is known that the two  $\alpha$ -apoprotein tyrosines ( $\alpha$ -Tyr 44, 45) are important B850-binding sites of

BChl-B850 [49]. It was reported that the presence of different carotenoid termini in LH2 influences the hydrogen bonding between  $\alpha$ -Tyr 44, 45 and the BChl-B850 using FT-Raman measurement [50]. A plausible explanation is that the perturbation of the protein structure may be induced by the change of the carotenoid polar group. However, based on our results, losing the carotenoid polar group does not influence the lifetime of the B850 excited singlet state.

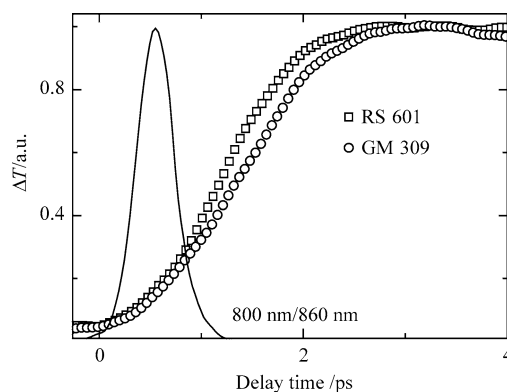


**Fig. 12** Normalized two color fs pump-probe dynamics of the native LH2 and GM 309 at a probe wavelength of 860 nm and excitation at 800 nm. The cross correlation trace between the excitation pulse and the probe pulse is also given in the figure.

## 6 The effect of electrochemical oxidation on the energy transfer within the LH2 complex

As crucial species directly participating in the ultrafast photo-induced excitation relaxation, BChls are treated as the main objects for probing the structural properties and primary events in both the antenna complexes and RC of the photosynthetic bacteria. A great deal of work has focused on the effect of BChl oxidation on the structural characterization and the energy transfer mechanism by using the steady [51–54] and time-resolved absorption [27, 55–57], fluorescence emission [53, 55, 58], circular dichroic and electron paramagnetic resonance (EPR) [59–61]. Among all these works, monitoring of the fluorescence quenching enables the direct and clear observation of the change of energy transfer, which is in tight connection with the BChl oxidation process [53, 55, 58]. Generally speaking, the loss of fluorescence is mainly due to the trapping of excitation energy somewhere in the photosynthetic units. In most cases, trapping of excitation in molecular aggregates occurs if an impurity has an excited state energy level lower than that of the aggregates [53, 55, 62–66]. Therefore, the BChls radical cation, which has an optical absorption band reported near 925 nm [67–69], could act as such an impurity for effectively trapping the excitation energy in the bacteria photosynthetic units. In this section, we introduce the crucial dependence between the BChl radical cation generation with the pigment-protein arrangement and energy transfer in LH2 from *Rb sphaeroides*

601 for a comprehension of the detailed dynamical evolution of the competitive quenching pathway, which was generated by electrochemical oxidation of the LH2 complexes.

The electrochemical experiments were performed with steady absorption, steady fluorescence, and femtosecond pump-probe measurements adopted simultaneously. The well-designed spectroelectrochemical study of the BChl oxidation provides an effective way for in-situ probing the electrochemical-affected ultrafast energy transfer processes, which could hardly be derived from those traditional methods. The experimental results revealed that the BChl-B850 radical cation acted as an additional channel, rapid quenching the excitation energy with almost unchanged  $B800 \rightarrow B850$  energy transfer rate.

The electrochemical experiments were performed within a home-made, three-electrode spectroelectrochemical cell with optical path length  $\sim 1$  mm in the dark. Two homogeneous minigrad gold nets with surface area of  $1.6 \text{ cm}^2$  were used as the working electrode and auxiliary electrode, respectively. An Ag/AgCl wire was employed as the reference one. The gold electrode was washed successively with 1 M KOH in 60 % ethanol, deionized water, 2 M HCl, and then rinsed carefully with deionized water again for cleaning before each spectroelectrochemical experiment. A CHI-660A electrochemical workstation (CHI Instrument Co., USA) was employed for conducting the electrochemical experiments. The potentials presented in this paper were vs. the standard hydrogen electrode (SHE).

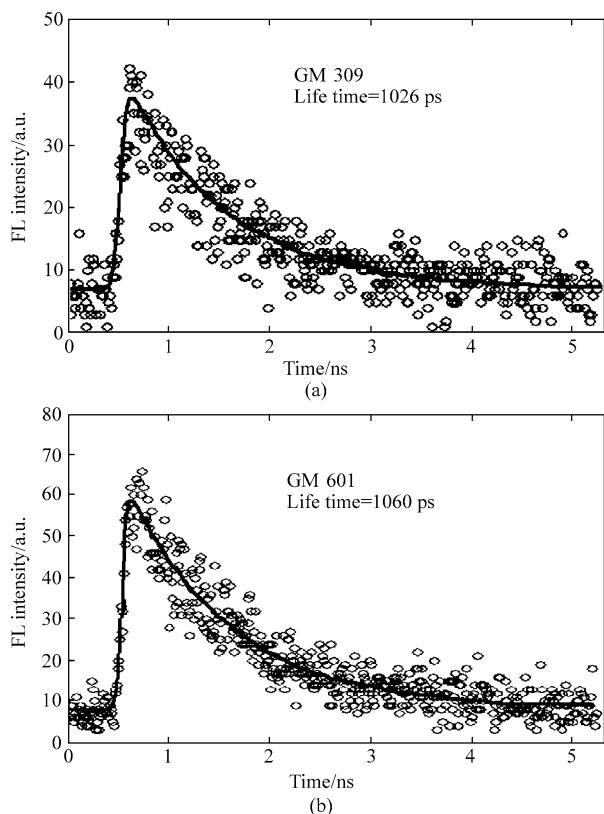


**Fig. 13** Time-resolved fluorescence emission from B850 : (a) GM 309 and (b) native LH2.

The optically transparent cell for spectroelectrochemical experiments was placed properly in the fs pump-probe system. Two SM-240 CCD spectrophotometers were also established suitably in the system for achieving the real-time detecting of the oxidation process (see inset of Fig. 14). The absorption, fluorescence emission, and fs pump-probe were measured during the oxidation with three independent computers. All light beams were blocked after each measurement to avoid the possible photo-oxidation.

Firstly, NIR-absorption-monitored electrochemical experiments were carried out to probe the oxidation behavior of the BChls in LH2. At redox potential higher than 0.8 V, obvious spectral changes of both the B800 and B850 bands indicate clearly the BChl oxidation. The detailed effect of in-situ electrochemical oxidation (at the potential of  $\sim 0.8$  V) on the BChl absorption of LH2 is demonstrated in Fig. 14. The BChl oxidation results in bleaching of both the B800 and B850  $Q_y$  bands accompanied with a slight red shift of the B850 band from 850 nm to 855 nm. With the continuously applied potential ( $\sim 0.8$  V), the B800 absorption peak completely disappears 30 minutes later, whereas the B850 absorption peak still keeps  $\sim 40$  % of its original absorbance. Meanwhile, a new absorption peak emerges at 685 nm, which is probably due to the formation of the BChl dication ( $BChl^{2+}$ ) [51]. The absorption spectra recorded at different oxidation time reveal a bleaching of both the  $Q_y$  bands of B800 and B850. Interestingly, although the degradation of both B800 and B850  $Q_y$  bands takes place at practically the same potential, the B800 band bleaches faster than the B850 band [52], which indicates that the ring structure of the monomeric BChl-B800 is more incompact than the dimeric BChl-B850. The observed concomitant slight red shift of B850 band (from 850 nm to 855 nm) is likely attributed to the changes of BChl-protein and BChl-BChl interaction, which arise from the minor changes in distance between the pigment molecules [70–72] and/or the changes in hydrogen bonding between the protein and the pigment [73, 74] upon the electrochemical oxidation. Moreover, the loss of BChl-B800 caused by electrochemical oxidation may also bring the BChl-B850 band to a slight red shift, as is similar to the observation upon selective removal of the BChl-B800 from the native LH2 [11, 75].

Figure 15 (a) shows the evolution of the fluorescence emission spectra (under excitation of 800 nm beam) during the electrochemical oxidation. Distinct quenching of fluorescence emission occurs immediately while the electrochemical oxidation starts. The relationship between the change of the absorbance as well as fluorescence emission with the time for electrochemical oxidation of LH2 is shown in Fig. 15 (b). Remarkable decrease of fluorescence intensity is observed as compared with the bleaching of both B800 and B850 absorption bands at the same experimental condition. A 50 % loss of the original fluorescence intensity is observed after 6 min oxidation, while only 5 %–10 % reduction of the original absorbance of BChl (B800 and

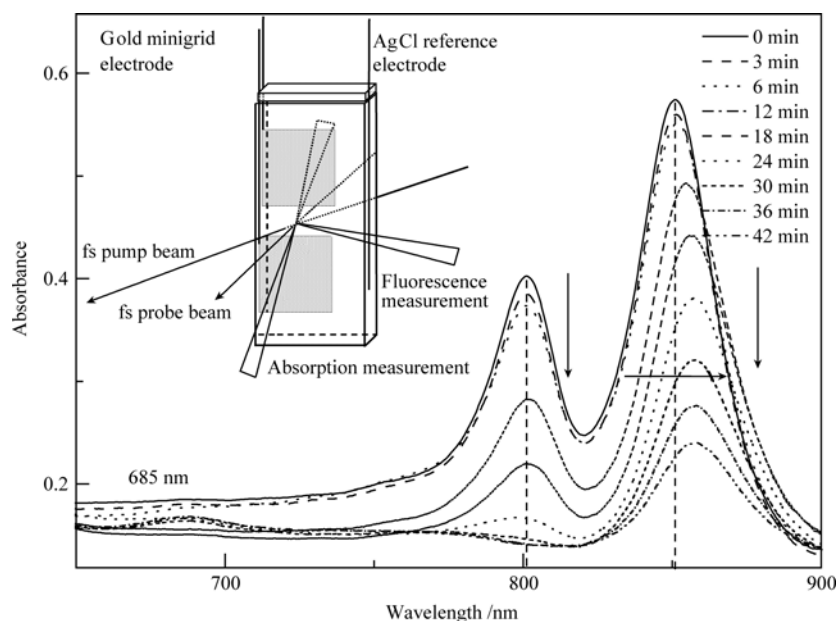


**Fig. 14** Effect of electrochemical oxidation on the time-dependent  $Q_y$  absorption of LH2. Inset displays the schematic view of the experimental setup for fs pump-probe spectroelectrochemical measurements at a homemade optically transparent cell. NIR absorption and fluorescence spectroelectrochemical experiments are also established in the system for the real-time monitor of the oxidation process.

B850) is acquired. As the oxidation goes on, the fluorescence emission is completely quenched about 20 min later, however, the absorbances of B800 and B850 bands still keep 30 % and 70 % of the original value, respectively. Electrochemical oxidation of LH2 dramatically quenches the fluorescence emission from B850, demonstrating that oxidation of few BChl molecule within the B800 ring and the B850 ring is sufficient to produce  $\sim 50\%$  quenching of the fluorescence intensity. This phenomenon is well consistent with the results obtained from photooxidation of LH2 from *Rps. Acidophila* [55] and chemical oxidation of LH1 from *Rh. Marinum* [53]. It appears that the presence of a single oxidized BChl molecule in the BChl-B850 ring could effectively quench the fluorescence originating from the excitation of B800 ring [55], yet the degradation of BChl-B800 is certainly not the key factor to the fluorescence quenching. When the fluorescence emission is completely quenched, the absorption peak of BChl-B800 still keeps 30 % of the original absorbance [see Fig. 15 (b)].

One color fs pump-probe experiment results of the LH2 excited at 800 nm during the electrochemical oxidation process are given in Fig. 16. For the unoxidized LH2, the initial dynamics exhibits an ultrafast decay of the PB, and an additional PA attributed to the excited state absorption of the B850 band. With BChl oxidation taking place, a significant disappearance of the PA signal is observed 6 min later. Then, a new PB signal with long lifetime and gradually increased magnitude is observed. Eventually, the dynamics evolution of B800 is mainly dominated by the long lifetime PB signal. The corresponding fitting results reveal that the fast decay time component of 0.65 ps, which mainly reflects the rate of energy transfer from B800 to B850 [28], is nearly independent on the electrochemical oxidation.

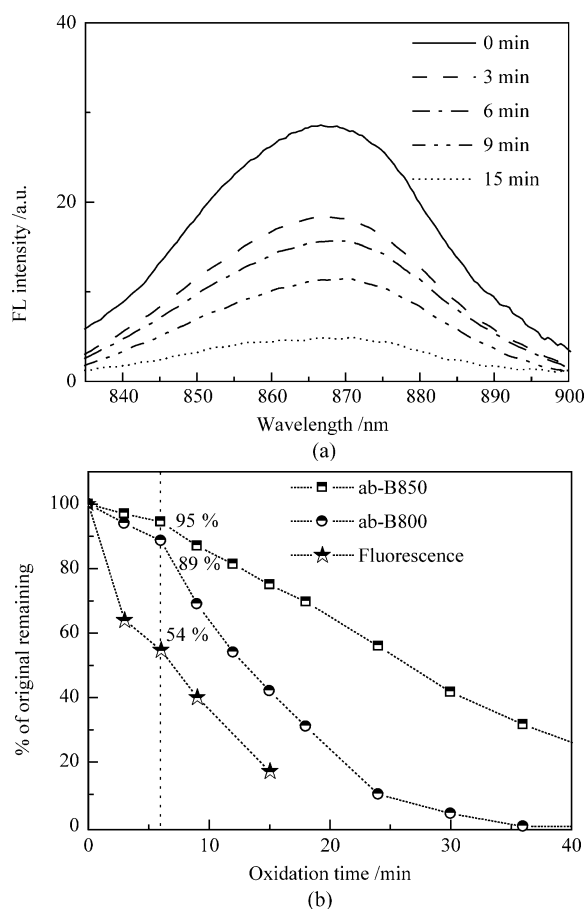


**Fig. 15** (a) Effect of electrochemical oxidation on the fluorescence emission of LH2 at different oxidation time. (b) Comparison of the time-dependent changes of the BChl  $Q_y$  band absorption and fluorescence emission intensity of LH2 during electrochemical oxidation.

Upon electrochemical oxidation of the native LH2, the rate of B800–B850 energy transfer is nearly unchanged during the electrochemical oxidation. It has been suggested that the nearest B800–B800 neighborhood excitonic coupling is very weak, and therefore the B800 excitation is considered to be highly localized on the individual B800 molecule [76]. Accordingly, oxidation of the BChl-B800 molecules does not affect greatly the excitation energy transfer from the unoxidized BChl-B800 molecules to the B850 ring. On the other hand, the oxidized BChl-B850 molecules, though quenching the excitation energy efficiently, seem to also have minor effect on the B800–B850 energy transfer rate [27]. Moreover, although the B800–B850 energy transfer rate is not affected strongly by the electrochemical oxidation, a disappeared PA signal accompanied with a long-life PB signal generated is clearly observed. The PA signal is mainly attributed to the excited state absorption of the B850 band [see Fig. 4 (a)]. Thus, it is proposed that some other signals may be mixed in this dynamics upon the electrochemical oxidation, that is, the BChl radical cation in the B850 ring may act as an additional energy transfer channel to effectively quench the excitation energy. Such pathway may compete with the original energy transfer channel for trapping the excitation energy. At oxidation time of 6 min, the fact that 50 % of fluorescence quenching occurs in comparison with the  $\sim 10\%$  of BChl-B800 absorbance reduction reflects that almost half of the excitation energy is trapped by the BChl-B850 radical cation. The corresponding dynamical evolution shows a mono-exponential decay process, which may be ascribed to the overlapping of the PA and PB signals. As the oxidation goes on, the propor-

tion of BChl-B850 radical cation increases gradually, which enhances the trapping of excitation energy through such radical cation, and thus makes the increased PB signal to dominate the dynamics. At oxidation time of 20 min, the dynamics primarily reflects the excitation energy trapping process conducted by the BChl-B850 radical cation.

The pump-probe experiments of the LH2 conducted at 850 nm also clearly demonstrate the effect of electrochemical oxidation on the excited B850 dynamic process, as displayed in Fig. 16. For the unoxidized LH2, three time components of  $\sim 200$  fs,  $\sim 2$  ps, and  $> 100$  ps were achieved by data fitting, which reflects the intra/interband energy transfer pathways in the B850 ring [28]. The applied potential induces a stepwise decrease of the signal intensity and a dramatic change of dynamics depending on the oxidation time. After 20 min oxidation, the dynamics evolution of B850 shows a bi-exponential decay process with time constants of  $< 100$  fs and  $\sim 100$  ps.

The characteristic changes in B850 dynamics also indicate that an additional channel generated by oxidation of BChl-B850 molecules acts as the excitation energy trapping pathway. Fitting results for unoxidized LH2 exhibit a tri-exponential decay process. At oxidation time of 20 min, the completely quenched fluorescence reflects that the excitation energy is likely to be mostly trapped by the BChl-B850 radical cation, and the correspondent dynamics is predominated by bi-exponential decay processes. The decay time of the initial ultrafast process ( $< 100$  fs) is faster than that of the unoxidized LH2 and is beyond the resolution of the apparatus. Such ultrafast process observed may be interpreted as a time-scale of the quenching process between the

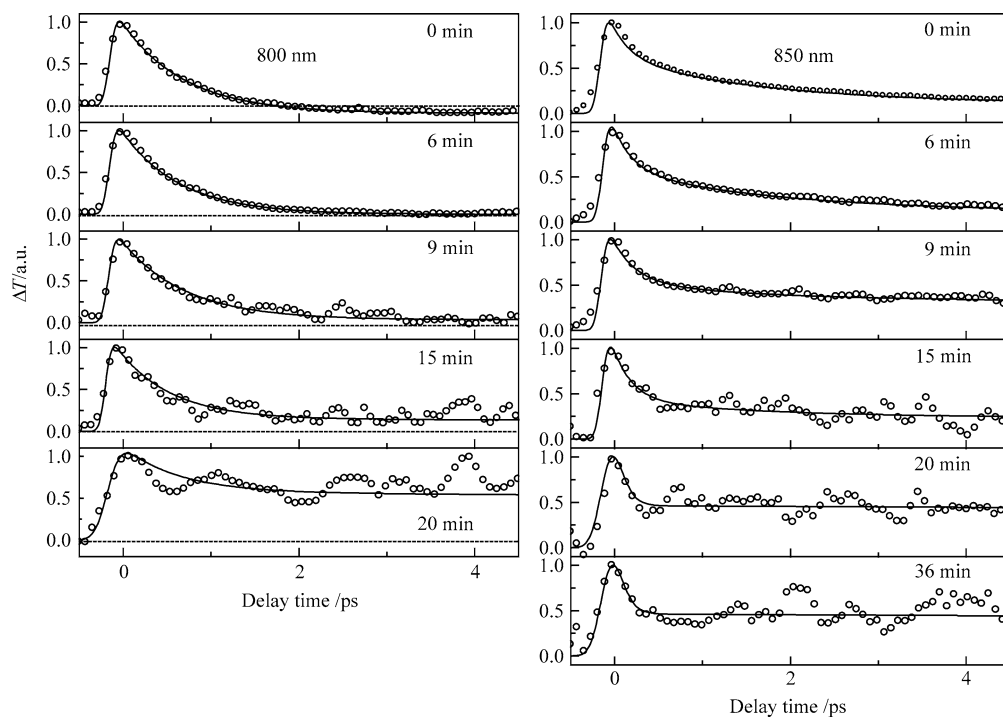


**Fig. 16** Effect of electrochemical oxidation on the time-dependent one-color fs pump probe for LH2 excited at 800 nm and 850 nm. The solid lines represent the fitting results.

excited BChl-B850 and the BChl-B850 radical cation, which is fast enough to compete with the original intracomplex excited state dynamics and energy transfer within LH2 [66, 77]. The 100 ps component could be probably ascribed to the lifetime of the B850 radical cation [57].

Figure 17 shows the proposed schemes of the excitation energy relaxation processes in the electrochemical oxidized LH2 complex. Compared with that of the unoxidized LH2 complex [see Fig. 17 (a)], the oxidation may induce the generation of a new energy levels from the BChl-B850 radical cation [see Fig. 17 (b)], which might act as an additional quenching energy channel to compete with the original BChl-B850 relaxation channel for trapping the excitation energy. After 20 min oxidation, the relaxation of excitation energy from the original channel is completely blocked, while only the channel produced by the BChl-B850 radical cation plays the key role of energy trapping pathway.

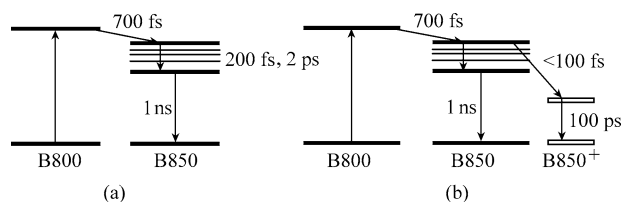


**Fig. 17** Proposed energetic diagrams of main transitions and relaxations in LH2 under the condition of unoxidation or oxidation. **(a)** The energy relaxation process of unoxidized LH2; **(b)** the energy relaxation process of oxidized LH2 during the oxidation time of twenty minutes.

## 7 Summary

In this paper, we introduce the comparison of dynamical evolution between the native LH2 and some mutated or treated LH2 complexes which include the B800 completely deleted LH2, carotenoid mutated LH2 and electrochemical oxidation treated LH2. Based on these researches, the energy transfer processes among the different pigments in the light-harvesting complex of purple bacteria are well elucidated. The LH2 complex can be considered as a donor-bridge-acceptor system where bacteriochlorophylls and carotenoid have interaction and play important roles in the energy transfer mechanism of LH2 complexes.

The understanding of the function of these pigments in the light-harvesting systems may inspire researchers to design and synthesize artificial multichromophoric molecular optical devices [78, 79], such as photonic wires [78], which can be optimized for efficient and rapid transfer of excited state energy over large distances. Additionally, the on/off switching control of the fluorescence might be accomplished by deactivation of the quencher or change of the interaction geometry between the chromophore and quencher [80], which could act as a photoswitch to introduce a controllable and highly efficient competing pathway in the photonic

wire [78].

## References

1. Van Grondelle R., Dekker J. P., Gillbro T., and Sundström V., *Biochim. Biophys. Acta*, 1994, 1187: 1
2. Fleming G. R., and van Grondelle R., *Physics Today*, 1994, 47(2): 48
3. Fleming G. R., and van Grondelle R., *Current Opinion in Structural Biology*, 1997, 7: 738
4. van Amerongen H., Valkunas L., and van Grondelle R., *Photosynthetic EXCITONS*, chapter 1. Published by World Scientific, 2000
5. Qian S. X., and Zhu R. Y., *Nonlinear Optics*, Chapter 10, Shanghai: Fudan university Press
6. McDermott G., Prince S. M., Freer A. A., Hawthornthwaite-Lawless A. M., Papiz M. Z., Cogdell R. J., and Isaacs N. W. *Nature*, 1995, 374: 517
7. Prince S. M., Papiz M. Z., Freer A. A., McDermott G., Hawthornthwaite-Lawless A. M., Cogdell R. J., and Isaacs N. W., *J Mol. Biol.*, 1997, 268: 412
8. Karrasch S., Bullough P. A., and Ghosh R., *EMBO. J.*, 1995, 14: 631
9. Sauer K., Cogdell R. J., Prince S.M., Freer A. A., Isaacs N. W., and Scheer H., *Photochem. Photobiol.*, 1996, 64: 564
10. Krueger B. P., Scholes G. D., and Fleming G. R., *J. Phys. Chem. B*, 1998, 27: 5378
11. Koolhaas M. H. C., Freese R. N., Fowler G. J. S., Bibby T.S., Georgakopoulou S., van der Zwan G., Hunter C. N., and van Grondelle R., *Biochemistry*, 1998, 37: 4693
12. Liu Y., Wu Y. Q., and Xu C. H., *Biochem. Bioph. Res. Co*, 2004, 325: 600
13. Herek J. L., Polivka T., Sundstrom V., and Stiel H., *Phys. Rev. Lett.*, 2001, 86: 4167
14. Pullerits T., Hess S., Herek J. L., and Sundstrom V., *J. Phys. Chem., B* 1997, 101: 10560
15. Scholes G. D., Harcourt R. D., and Fleming G. R., *J. Phys. Chem., B* 1997, 101: 7302
16. Pullerits T., Chachivilis M., Jones M. R., Hunter C. N., and Sundstrom V., *Chem. Phys. Lett.*, 1994, 22: 355
17. Koolhaas M. H. C., Van der Zwan G., Freese R. N., and Van Grondelle R., *J. Phys. Chem. B.*, 1997, 101: 7262
18. Ritz T., Hu X. H., Damjanovic A., and Schulten K. *J. Lumin.*, 1998, 16: 310
19. Hu X., Ritz T., Damjanovic A., and Schulten K., *J. Phys. Chem., B* 1997, 101: 3854
20. Nagarajan V., Alden R. G., Williams J. C., and Parson W. W., *Proc. Natl. Acad. Sci. USA*, 1996, 93: 13774
21. Polivka T., Pullerits T., Herek J. L., and Sundstrom V., *J. Phys. Chem., B* 2000, 104: 1088
22. Kumble R., Howard T. D., Cogdell R. J., and Hochstrasser R. M., *J. Photoch. Photobio., A* 2001, 142: 121
23. Nagarajan V., Johnson E. T., Williams J. C., and Parson W. W., *J. Phys. Chem., B* 1999, 103: 2297
24. Ihalainen J. A., Linnanto J., Myllyperkiö P., van Stokkum I. H. M., Ücker B., and Scheer H., Korppi-Tommola J. E. I., *J. Phys. Chem.,*

- B 2001, 105: 9849
25. Salverda J. M., van Mourik F., van der Zwan G., and van Grondelle R., *J. Phys. Chem.*, B 2000, 104: 11395
  26. Shreve A. P., Trautman J. K., Frank H. A., Owens T. G., and Albrecht A. C., *Biochem. Biophys. Acta.*, 1991, 1058: 280
  27. Monshouwer R., de Zarate I., van Mourik F., and van Grondelle R., *Chem. Phys. Lett.*, 1995, 246: 341
  28. Guo L. J., Liu Y., Yang Y., Mi J., Xu C., Xu C.H., and Qian S.X., *FEBS Letters*, 2002, 511: 69
  29. Monshouwer R., abrahamsson M., van Mourik F., and van Grondelle R., *J. Phys. Chem.*, B 1997, 101: 7241
  30. Matsuzaki S., Zazubovich V., Fraser N. J., Cogdell R.J., and Small G. J., *J. Phys. Chem.*, B 2001, 105: 7049
  31. Wu H. M., Savikhin S., Reddy N. R. S., Jankowiak R., Cogdell R. J., Struve W. S., and Small G. J., *J. Phys. Chem.*, 1996, 100: 12022
  32. Leupold D., Stiel H., Ehlert J., Nowak F., Teuchner K., Voigt B., Bandilla M., Ücker B., and Scheer H., *Chem. Phys. Lett.*, 1999, 301: 537
  33. Gall A., Robert B., Cogdell R. J., Bellissent-Funel M., and Fraser N. J., *FEBS Lett.*, 2001, 491: 143
  34. Papizl Z. M., Prince S. M., Howard T., Cogdell R. J., and Isaacs N. W., *J. Mol. Biol.*, 2003, 326: 1523
  35. Liu W. M., Zhu R.Y., Xia C.A., Liu Y., Xu C. H., and Qian S. X., *CHIN.PHYS.LETT.*, 2003, 20: 2148
  36. Liu W. M., Liu Y., Yan Y. L., Liu K. J., Guo L. J., Xu C. H., and Qian S. X., *J. Biomol. struct. Dyn.*, 2006, 23: 529
  37. Cogdell R. J., and Frank H. A., *Biochim. Biophys. Acta*, 1987, 895: 895
  38. Polivka T., and Sundström V., *Chem. Rev.*, 2004, 104: 2021
  39. Lang H. P., and Hunter C. N., *Biochem. J.*, 1994, 298:197
  40. Andersson P. O., Cogdell R. J., and Gillbro T., *Chem. Phys.*, 1996, 210: 195
  41. Andersson P. O., Cogdell R. J., and Gillbro T., *Chem. Phys.*, 1996, 210: 195
  42. Kramer H. J. M., Van Grondelle R., Hunter N., Westerhuis W. H. J., and Amesz J., *Biochim. Biophys. Acta.*, 1984, 765: 156
  43. Scholes G. D., and Fleming G. R., *J. Phys. Chem.*, B 2000, 104: 1854
  44. Frank H. A., Desamero R. Z. B., Chynwat V., Gebhard R., van der Hoef I., Jansen F. J., Lugtenburg J., Gosztola D., and Wasielewski M. R., *J. Phys. Chem.*, A 1997, 101: 149
  45. Fujii R., Onaka K., Kuki M., and Koyama Y., *Chem. Phys. Lett.*, 1998, 288: 847
  46. Kilså K., Kajanus J., Mårtensson J., and Albinsson B., *J. Phys. Chem.*, B 1999, 103: 7329
  47. Scholes G. D., Ghiggino, K. P., Oliver A. M., and Paddon-Row M. N., *J. Am. Chem. Soc.*, 1993, 115: 4345
  48. Liu W. M., Liu Y., Guo L. J. Xu C. H., and Qian S. X., *J. Lumin.*, 2006, 119: 350
  49. Fowler G. J. S., Visschers R. W., Grief G. G., van Grondelle R., and Hunter C. N., *Nature*, 1992, 355: 848
  50. Gall A., Cogdell R. J., and Robert B., *Biochemistry*, 2003, 42: 7252
  51. Kropacheva T. N., and Hoff A. J., *J. Phys. Chem.* B 2001, 105:5536
  52. Picorel R., Lefebvre S. and Gingras G., *Eur. J. Biochem.*, 1984, 142: 305
  53. Law C. J., and Cogdell R., *J. FEBS. Lett.*, 1998, 432: 27
  54. Rafferty C. N., Bolt J., Sauer K., and Clayton R. K., *Proc. Natl. Acad. Sci. USA*, 1979, 76: 4429
  55. Liu W. M., Lu Y. D., Liu Y., Liu K. J., Yan Y. L., Kong J. L., Xu C. H., and Qian S. X., *Biochem. Bioph. Res. Co.*, 2006, 340: 505
  56. Pšenčík J., Polivka T., Němec P., Dian J., Kudrna J., Malý P., and Hála J., *J. Phys. Chem. A.*, 1998, 102: 4392
  57. Bergström H., Sundström V., van Grondelle R., Åkesson E., and Gillbro T., *Biochim. Biophys. Acta.*, 1986, 852: 279
  58. Brune D. C., King G. H., Infosino A., Steiner T., Thewalt M. L. W., and Blankenship R. E., *Biochemistry*, 1987, 26: 8652
  59. Gomez I., Sieiro C., Ramirez J. M., Gomea-Amores S., and del Campo F., *J. FEBS. Lett.*, 1982, 144: 17
  60. Gomez I., Picorel R., Ramirez J. M., Perez R., and del Campo F. F., *Photochem. Photobiol.*, 1982, 35: 399
  61. Limantara L., Fujii R., Zhang J. P., Kakuno T., Hara H., Kawamori A., Yagura T., Cogdell R. J., and Koyama, Y. sphaeroides., *Biochemistry*, 1998, 15: 17469
  62. Wang J., Gosztola D., Ruffle S. V., Hemann C., Seibert M., Wasielewski M. R., Hille R., Gustafson T. L., and Sayre R. T., *Proc. Natl. Acad. Sci. USA*, 2002, 99: 4091
  63. Barzda V., Vengris M., Valkunas L., van Grondelle R., and van Amerongen, H. *Biochemistry*, 2000, 39:10468
  64. Rajagopal S., Egorova E. A., Bukhv N. G., and Carpentier R., *Biochim. Biophys. Acta.*, 2003, 1606: 147
  65. Hartwich G., Friese M., Scheer H., Ogrodnik A., and Michel -Beyerle M. E., *Chem. Phys.*, 1995, 197: 423
  66. Fiedor L., Scheer H., Tschirschwitz F., Ehlert J., Nibbering E., Leupold D., and Elsaesser T., *Chem. Phys. Lett.*, 2000, 319: 145
  67. Chauvet J. P., Vlovy R., Santus R., and Land E. J., *J. Phys. Chem.*, 1981, 85: 3449
  68. Fajer J., Borg D. C., Forman A., Felton R. H., Dolphin D., and Vegh L., *Proc. Natl. Acad. Sci. USA*, 1974, 71: 994
  69. Fuhrhop J. H., and Mauzerall D., *J. Am. Chem. Soc.*, 1969, 91: 4174
  70. Sturgis J. N., Gall A., Ellervee A., Freiberg A., and Robert B., *Biochemistry*, 1998, 37: 14875
  71. Timpmann K., Ellervee A., Pullerits T., Ruus R., Sundström V., and Freiberg A., *J. Phys. Chem.*, B 2001, 105: 8436
  72. Gall A., Ellervee A. Sturgis, J. N., Fraser N. J., Cogdell R. J., Freiberg A., and Robert B., *Biochemistry*, 2003, 42: 13019
  73. Kwa L. G., Garcia-Martin A., Vègh A. P., Strohmman B., RobeRt B., and Braun P., *J. Biol. Chem.*, 2004, 279: 15067
  74. Buche A., Ramirez J. M., and Picorel, R. *Eur. J. Biochem.*, 2000, 267: 3235
  75. Bandilla M., Ucker B., Ram M., Simonin I., Gelhaye E., McDermott G., Cogdell R. J., and Scheer H., *Biochim. Biophys. Acta.*, 1998, 1364: 390
  76. Sundström V., Pullerits T., and van Grondelle R. J., *J. Phys Chem.*, B 1999, 103: 2327
  77. Fiedor L., Leupold D., Teuchner K., Voigt B., Hunter C. N., Scherz A., and Scheer H. *Biochemistry*, 2001, 40: 3737
  78. Tinnefeld P., Heilemann M., and Sauer M., *ChemphysChem.*, 2005, 6:217
  79. Irie M., Fukaminato T., Sasaki T., Tamai N., and Kawai T. *nature*, 2002, 420: 759
  80. liang Y. C., Dvornikov A. S., and Rentzepis P. M., *Proc. Natl. Acad. Sci. USA*, 2003, 100: 8109